ISSN 1726-5749

SENSORS & TRANSDUCERS

vol. 7 Special 10 /09

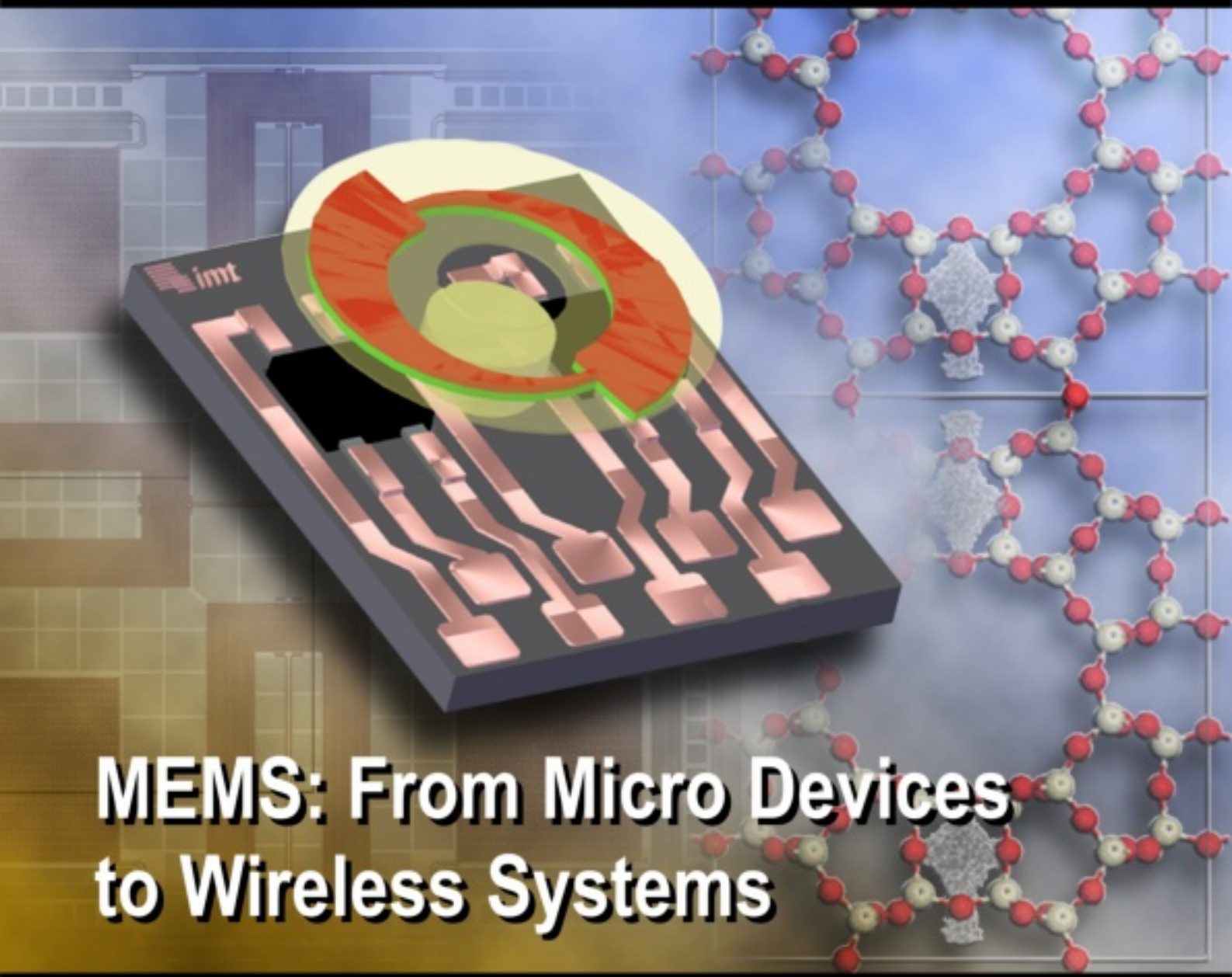

MEMS: From Micro Devices to Wireless Systems

International Frequency Sensor Association Publishing

IFSA

Sensors & Transducers

Volume 7, Special Issue, October 2009

www.sensorsportal.com

ISSN 1726-5479

Editors-in-Chief: professor Sergey Y. Yurish,
Phone: +34 696067716, fax: +34 93 4011989, e-mail: editor@sensorsportal.com
Guest Editors: Dr. Elena Gaura and Dr. James P. Brusey

Sensors & Transducers Journal (ISSN 1726-5479) is a peer review international journal published monthly online by International Frequency Sensor Association (IFSA).
Available in electronic and on CD.

Sensors & Transducers Journal

Contents

Volume 7
Special Issue
October 2009

www.sensorsportal.com

ISSN 1726-5479

Research Articles

Authors are encouraged to submit article in MS Word (doc) and Acrobat (pdf) formats by e-mail: editor@sensorsportal.com
Please visit journal's webpage with preparation instructions: http://www.sensorsportal.com/HTML/DIGEST/Submition.htm

Sensors & Transducers Journal, Vol. 7, Special Issue, October 2009, pp. 88-100

www.sensorsportal.com

Sensors & Transducers

ISSN 1726-5479

http://www.sensorsportal.com

Application of Nonlocal Elasticity Shell Model for Axial Buckling of Single-Walled Carbon Nanotubes

[*]Farzad Khademolhosseini, [+]Nimal Rajapakse, [*]Alireza Nojeh

[*]The University of British Columbia, Vancouver, Canada

[+]Simon Fraser University, Burnaby, Canada

[*]Tel.: 1-604-8220939

E-mail: khadem@interchange.ubc.ca

Received: 28 August 2009 /Accepted: 28 September 2009 /Published: 12 October 2009

Abstract: Recently, nano devices have been developed which use Carbon Nanotubes (CNTs) as structural elements. To define the range of applicability of CNTs in such devices, it is important to investigate failure modes such as the axial buckling limit. Classical continuum models are inaccurate as they are unable to account for the size-effects in such devices. In this work, a modified nonlocal continuum shell model for the axial buckling of CNTs is proposed and compared with a nonlocal model for torsional buckling. This is done through modifying classical continuum models by incorporating basic concepts from nonlocal elasticity. Furthermore, molecular dynamics (MD) simulations are performed on a range of nanotubes with different diameters. Compared to classical models, the modified nonlocal models provide a much better fit to MD simulation results. Using MD simulation results for axial buckling, values of the nonlocal constant and shell thickness are calculated.

Keywords: Carbon nanotube, Buckling, Nonlocal elasticity, Shell, Molecular dynamics

1. Introduction

Carbon nanotubes (CNTs) have been the subject of ongoing research. These interesting nano-structures exhibit superior mechanical, electrical, thermal, magnetic and optical properties, and could provide the means for development of novel devices at the nanoscale. Ever since their discovery, much work has been done on the characterization and modeling of CNT properties, ranging from experimental observations to numerical simulations. Among the different approaches, continuum modeling is of special interest in defining the mechanical properties of CNTs. Continuum models are

simple and efficient, however, in their classical form, they are unable to account for the size-effects that arise due to the discrete nature of matter at the nanoscale. To overcome such problems, modified continuum models have been proposed. One such model is based on the nonlocal elasticity theory proposed by Eringen [1-3], which has recently been successfully used to show size effects in nanoscale structures [4]. Using the same approach, in this paper, a modified nonlocal continuum shell model for the buckling of carbon nanotubes is proposed to account for the size effects and provide an efficient and accurate method for the prediction of CNT properties. The proposed shell model is validated through comparison with results from molecular dynamics simulations, and consistent values for the shell thickness and nonlocal elasticity constant of nanotubes are determined.

2. Nonlocal Elasticity Shell Model

In this section, the basic concepts of nonlocal elasticity as proposed by Eringen in the 1970's [1, 2] are briefly presented. These basic equations are used to develop a nonlocal elasticity shell model to predict the axial buckling load of single-walled carbon nanotubes (SWCNTs).

2.1. Nonlocal Theory of Elasticity

This theory states that the stress at a reference point X in a body depends not only on the strain at point X, but also on the strains at all other points X' in the body [3]. The basic equations of the nonlocal elasticity theory are [3];

$$\begin{aligned}
&\sigma_{kl,k} + \rho(f_l - \ddot{u}_l) = 0 \\
&\sigma_{kl}(x) = \int_V \alpha\left(|x - x'|, \tau\right)\sigma^c_{kl}(x')dv(x') \\
&\sigma^c_{kl}(x') = \lambda e_{rr}(x')\delta_{kl} + 2\mu e_{kl}(x') \\
&e_{kl}(x') = \frac{1}{2}\left(\frac{du_k(x')}{dx'_l} + \frac{du_l(x')}{dx'_k}\right)
\end{aligned} \tag{1}$$

where σ_{kl}, ρ, f, u_l are the stress tensor, mass density, body force density and the displacement vector at x respectively. $\sigma^c_{kl}(x')$ is the classical stress tensor at x' which is related to the linear strain tensor $e_{kl}(x')$ at point x' through Lame constants λ and μ. The kernel function $\alpha(|x'- x|,\tau)$ is the nonlocal modulus and $|x'- x|$ is the Euclidean distance between points x' and x, $\tau=e_0d/l$, where d is an internal characteristic length of the system (such as the carbon-carbon bond length), l is an external characteristic length (such as the CNT radius or the CNT length) and e_0 represents Eringen's nonlocal elasticity constant which has to be determined for each material independently.

For a special class of physically admissible kernels, the above integro-partial differential equations of nonlocal elasticity can be reduced to singular partial differential equations. In the case of homogenous, isotropic elastic bodies the above equations reduce to:

$$(1 - e_0^2 d^2 \nabla^2)\sigma = C_0 : \varepsilon\,, \tag{2}$$

where C_0 is the elastic stiffness tensor of classical (local) isotropic elasticity, σ is the nonlocal stress tensor, ε is the strain tensor and ':' denotes the inner product of tensors [5].

2.2. Modified Timoshenko Shell Model for Axial Buckling

In this approach a CNT is modeled as a thin cylindrical shell with thickness h and radius a. A cylindrical coordinate system (r, θ, x) is used with the x axis along the centre of the cylinder and r *and* θ corresponding to the radial and circumferential directions, respectively (Fig. 1).

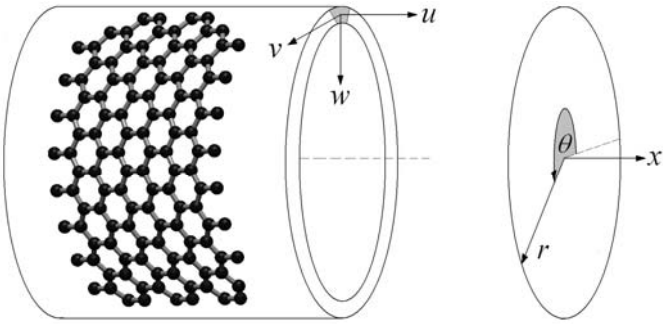

Fig. 1. Cylindrical shell representation of a SWCNT with the coordinate system used.

The displacements in the axial, circumferential and radial directions of the shell denoted by u, v and w, respectively are functions of only x and θ. Note that these are small displacements measured from the compressed equilibrium state of the shell just prior to axial buckling. The non-zero strains due to axial buckling can be expressed in terms of displacements as [6];

$$\begin{aligned} \varepsilon_{xx} &= \frac{du}{dx} \\ \varepsilon_{\theta\theta} &= \frac{1}{a}\frac{dv}{d\theta} - \frac{w}{a} \\ \varepsilon_{x\theta} &= \frac{1}{2}\left(\frac{1}{a}\frac{du}{d\theta} - \frac{dv}{dx}\right) \end{aligned} \tag{3}$$

Based on equation (2), the nonlocal form of Hooke's law for the stress-strain relations in a cylindrical coordinate system can be expressed in the following form;

$$\begin{aligned} \sigma_{xx} - \xi\ \nabla_R^2\sigma_{xx} &= \frac{E}{1-\upsilon^2}\left(\varepsilon_{xx} + \upsilon\varepsilon_{\theta\theta}\right) \\ \sigma_{\theta\theta} - \xi\ \nabla_R^2\sigma_{\theta\theta} &= \frac{E}{1-\upsilon^2}\left(\varepsilon_{\theta\theta} + \upsilon\varepsilon_{xx}\right)\ , \\ \sigma_{x\theta} - \xi\ \nabla_R^2\sigma_{x\theta} &= \frac{E}{1+\upsilon}\varepsilon_{x\theta} \end{aligned} \tag{4}$$

where

$$\nabla_R^2 = \frac{d^2}{dx^2} + \frac{1}{a^2}\frac{d^2}{d\theta^2} \quad , \quad \xi = (e_0 d)^2 \tag{5}$$

ξ is the nonlocal parameter, and E and υ are the Young's modulus and Poisson's ratio respectively.

Substitution of equation (3) into equation (4) and integration over a cross-sectional element of unit width yields:

$$\begin{aligned} N_{xx} - \xi\ \nabla_R^2 N_{xx} &= \frac{Eh}{1-\upsilon^2}\left(\frac{du}{dx} + \upsilon\left(\frac{1}{a}\frac{dv}{d\theta} - \frac{w}{a}\right)\right) \\ N_{\theta\theta} - \xi\ \nabla_R^2 N_{\theta\theta} &= \frac{Eh}{1-\upsilon^2}\left(\frac{1}{a}\frac{dv}{d\theta} - \frac{w}{a} + \upsilon\frac{du}{dx}\right) \\ N_{x\theta} - \xi\ \nabla_R^2 N_{x\theta} &= \frac{Eh}{2(1+\upsilon)}\left(\frac{1}{a}\frac{du}{d\theta} + \frac{dv}{dx}\right) \end{aligned} \tag{6}$$

$$\begin{aligned} M_{xx} - \xi\ \nabla_R^2 M_{xx} &= -\frac{Eh^3}{12a(1-\upsilon^2)}\left(\frac{d^2w}{dx^2} + \frac{\upsilon}{a^2}\left(\frac{d^2w}{d\theta^2} + \frac{dv}{d\theta}\right)\right) \\ M_{\theta\theta} - \xi\ \nabla_R^2 M_{\theta\theta} &= -\frac{Eh^3}{12a(1-\upsilon^2)}\left(\upsilon\frac{d^2w}{dx^2} + \frac{1}{a^2}\left(\frac{d^2w}{d\theta^2} + \frac{dv}{d\theta}\right)\right), \\ M_{x\theta} - \xi\ \nabla_R^2 M_{x\theta} &= \frac{Eh^3}{12a(1+\upsilon)}\left(\frac{dv}{dx} + \frac{d^2w}{dxd\theta}\right) \end{aligned} \tag{7}$$

where *Nij* (*i*, *j*= *x*, *θ*) is the force per unit length and *Mij* (*i*, *j*= *x*, *θ*) is the moment per unit length on a cross section of the shell respectively; and *h* is the shell thickness (Fig. 2).

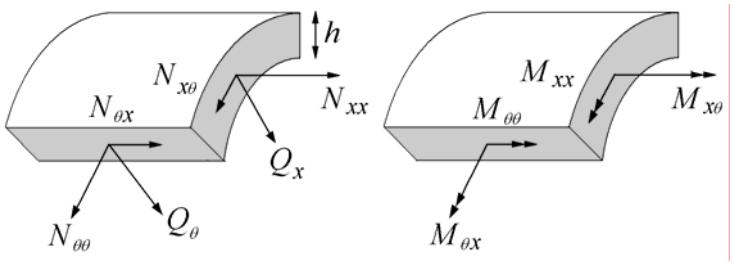

Fig. 2. Definition of forces and moments per unit length acting on a shell.

For the case of buckling of a cylindrical shell under the action of uniform axial pressure it can be assumed that all resultant forces except N_x (resultant force acting on the shell cross-section in the axial direction) are small. The resulting equilibrium equations of forces in the system are [6]:

$$\begin{aligned} a\frac{dN_{xx}}{dx} + \frac{dN_{\theta x}}{d\theta} &= 0 \\ \frac{dN_{\theta\theta}}{d\theta} + a\frac{dN_{x\theta}}{dx} + aN_{xx}\frac{d^2v}{dx^2} - Q_\theta &= 0, \\ a\frac{dQ_x}{dx} + \frac{dQ_\theta}{d\theta} + aN_{xx}\frac{d^2w}{dx^2} + N_{\theta\theta} &= 0 \end{aligned} \tag{8}$$

where *Qi* (*i*=*x*, *θ*) denotes the shearing forces acting in the radial direction (Fig. 2). Equilibrium equations for the moments acting on the shell are [6]:

$$a\frac{dM_{x\theta}}{dx}-\frac{dM_{\theta\theta}}{d\theta}+aQ_{\theta}=0$$
$$a\frac{dM_{xx}}{dx}-\frac{dM_{\theta x}}{d\theta}-aQ_{x}=0 \tag{9}$$

Combining equations (8) and (9) the three equations of equilibrium for an axially compressed cylindrical shell are [6]:

$$a\frac{dN_{xx}}{dx}+\frac{dN_{\theta x}}{d\theta}=0$$
$$\frac{dN_{\theta\theta}}{d\theta}+a\frac{dN_{x\theta}}{dx}+aN_{xx}\frac{d^2v}{dx^2}+\frac{dM_{x\theta}}{dx}-\frac{dM_{\theta\theta}}{ad\theta}=0 \tag{10}$$
$$a\frac{d^2M_{xx}}{dx^2}+\frac{d^2M_{\theta\theta}}{d\theta^2}+\frac{d^2M_{\theta x}}{dxd\theta}+aN_{xx}\frac{d^2w}{dx^2}+N_{\theta\theta}-\frac{d^2M_{x\theta}}{dxd\theta}=0$$

Applying the $(1-\xi\nabla_R^2)$ operator on equation (10) and use of equations (6) and (7) yields the following modified governing differential equations for the axial buckling of a cylindrical shell;

$$\frac{d^2u}{dx^2}+\frac{1}{2}(1-\upsilon)\frac{d^2u}{a^2d\theta^2}+\frac{1}{2a}(1+\upsilon)\frac{d^2v}{dxd\theta}-\frac{\upsilon}{a}\frac{dw}{dx}=0 \tag{11.a}$$

$$\frac{1}{2}(1+\upsilon)\frac{d^2u}{dxd\theta}+\frac{1}{2}a(1-\upsilon)\frac{d^2v}{dx^2}+\frac{d^2v}{ad\theta^2}-\frac{dw}{ad\theta}+\alpha\left(\frac{d^2v}{ad\theta^2}+a(1-\upsilon)\frac{d^2v}{dx^2}+a\frac{d^3w}{dx^2d\theta}+\frac{d^3w}{ad\theta^3}\right)$$
$$-a\phi\left(\frac{d^2v}{dx^2}\right)+a\phi\xi\left(\frac{d^4v}{dx^4}+\frac{1}{a^2}\frac{d^4v}{dx^2d\theta^2}\right)=0 \tag{11.b}$$

$$\upsilon\frac{du}{dx}+\frac{dv}{ad\theta}-\frac{w}{a}-\alpha\left(a^3\frac{d^4w}{dx^4}+2a\frac{d^4w}{dx^2d\theta^2}+\frac{d^4w}{ad\theta^4}+(2-\upsilon)a\frac{d^3v}{dx^2d\theta}-\frac{d^3v}{ad\theta^3}\right)$$
$$-a\phi\left(\frac{d^2w}{dxd\theta}\right)+a\phi\xi\left(\frac{d^4w}{dx^4}+\frac{1}{a^2}\frac{d^4w}{dx^2d\theta^2}\right)=0 \tag{11.c}$$

where

$$\phi=\frac{N_{xx}(1-\upsilon^2)}{Eh},\quad \alpha=\frac{h^2}{12a^2} \tag{12}$$

For the general case of the axial buckling of a cylindrical shell with length l and radius a, the buckling displacements are of the following form [6];

$$u=A\sin n\theta\cos\frac{m\pi x}{l}$$
$$v=B\cos n\theta\sin\frac{m\pi x}{l} \tag{13}$$

$$w = C \sin n\theta \sin \frac{m\pi x}{l},$$

where m is the number of half waves along the cylinder axis and n is the number of waves in the circumferential direction.

It is important to note here that for n=0 symmetrical buckling occurs which coincides with radial expansion and compression of the tube. For n=1 the cross-section of the tube remains circular and the tube buckles as a strut [42]. None of these modes are of interest to the current work and from here on, only the shell-type axial buckling mode-shapes with n>1 are considered. Substitution of equations (13) into the modified governing differential equations (11) and solution of the resulting eigenvalue problem yields the following relation for the modified critical axial buckling load of a cylindrical shell:

$$F_{cr}^{NT} = \sigma_{cr}.2\pi ah = \frac{\frac{2\pi Eh^2}{\sqrt{3(1-\upsilon^2)}} \cdot \frac{n^2-1}{n^2+1}}{1+e_0^2 \frac{d^2}{a^2}(\lambda^2+n^2)}, \tag{14}$$

where $\lambda=m\pi a/l$. The non-dimensional form of the critical buckling load is

$$\bar{F}_{cr}^{NT} = \frac{F_{cr}^{NT}}{Eh^2} = \frac{\frac{2\pi}{\sqrt{3(1-\upsilon^2)}} \cdot \frac{n^2-1}{n^2+1}}{1+e_0^2 \frac{d^2}{a^2}(\lambda^2+n^2)} \tag{15}$$

For comparison the classical Timoshenko relations for the critical axial buckling load and its non-dimensional form are [6]:

$$\bar{F}_{cr}^{T} = \frac{F_{cr}^{T}}{Eh^2} = \frac{2\pi}{\sqrt{3(1-\upsilon^2)}} \cdot \frac{n^2-1}{n^2+1} \tag{16}$$

Therefore,

$$\frac{F_{cr}^{T}}{F_{cr}^{NT}} = \frac{\bar{F}_{cr}^{T}}{\bar{F}_{cr}^{NT}} = 1+e_0^2 \frac{d^2}{a^2}(\lambda^2+n^2) \tag{17}$$

Comparison of equations (15) and (16) clearly shows that the former is size-dependant. This size-dependency is further explained in the next section. Equations (14) and (15) are based on the critical axial buckling wavelength calculated as [6]:

$$\lambda^2 = \frac{hn^2(n^2-1)}{2a\sqrt{3(1-\upsilon^2)}} \tag{18}$$

It is interesting to compare the nonlocal buckling loads for axial buckling derived here with the nonlocal buckling torque for the case of torsional buckling derived previously by the authors [7]. For a single-walled carbon nanotube the nonlocal Timoshenko model for the buckling torque is [7]

$$\bar{M}_{cr}^{NT} = \frac{M_{cr}^{NT}}{E\sqrt{ah^5}} = \frac{\frac{\pi\sqrt{2}}{3(1-\upsilon^2)^{3/4}}}{1+e_0^2\frac{d^2}{a^2}(\lambda^2+n^2)} \tag{19}$$

and the non-dimensional form of the buckling torque corresponding to the classical thin shell model based on ideal elasticity is [6]

$$\bar{M}_{cr}^{T} = \frac{M_{cr}^{T}}{E\sqrt{ah^5}} = \frac{\pi\sqrt{2}}{3(1-\upsilon^2)^{3/4}} \tag{20}$$

Therefore,

$$\frac{\bar{M}_{cr}^{T}}{\bar{M}_{cr}^{NT}} = \frac{M_{cr}^{T}}{M_{cr}^{NT}} = 1+e_0^2\frac{d^2}{a^2}(\lambda^2+n^2) \tag{21}$$

It is important to note that for the case of torsional buckling λ^2 is small compared to n^2 and is sometimes omitted from equations (19) to (21). The results of equations (19) to (21) are based on the following critical buckling wavelength (λ_{cr}) given by Timoshenko and Gere [6]:

$$\lambda_{cr} = \sqrt{\frac{2h}{a\sqrt{(1-\upsilon^2)}}} \tag{22}$$

2.3. Size-dependency of Nonlocal Models

Looking back at the classical relations for buckling loads shown in equations (16) and (20) it is easily seen that the non-dimensional form of these buckling loads is independent of size. In other words, regardless of the geometric dimensions and aspect ratios of a cylindrical shell, classical models always predict the same value for the non-dimensional buckling load. In contrast, looking at the nonlocal forms of buckling loads derived in equations (15) and (19) it is easily seen that the non-dimensional form of these buckling loads is size-dependent. This is due to the presence of geometric ratios in the denominators of the aforementioned equations. As an example the denominator of equation (15) is analyzed here:

$$1+e_0^2\frac{d^2}{a^2}(\lambda^2+n^2) = 1+e_0^2\left(n^2\left(\frac{d}{a}\right)^2+m^2\pi^2\left(\frac{d}{l}\right)^2\right) \tag{23}$$

The magnitude of the expression of equation (23) depends on the value of two geometric ratios, d/a and d/l, where d is the inter-atomic distance or the C-C bond length and a and l are the radius and length of the CNT, respectively. Since d is constant or almost constant for all CNTs (d ≈ 1.41 angstroms), based on their respective length and diameter, different CNTs will have different d/a and d/l ratios and thus different non-dimensional buckling loads. As the lengths and diameters of CNTs become smaller and comparable to the inter-atomic distance d, the d/a and d/l ratios become larger and have a greater impact on the magnitude of equation (23). This is how nonlocal models are able to account for size-effects. The magnitude of the expression of equation (23) also depends on:

- The buckling mode-shape through the values of m (longitudinal half-wave number) and n (circumferential wave-number). As wave-numbers increase, the corresponding wavelengths decrease and become comparable to the inter-atomic distance d.
- The value of the nonlocal elasticity constant e_0, which has to be determined for each material independently.

Fig. 3, which is based on equations (17) and (21) gives a comparison of classical and nonlocal buckling loads for different values of the nonlocal constant e_0. It is seen that the value of the nonlocal constant can significantly affect the buckling loads predicted by the nonlocal models. The difference between classical and nonlocal models is significant for CNTs with small diameters, but this difference becomes negligible at larger diameters where the nonlocal and classical models converge.

Based on the above observations it is important to know the buckling mode-shape (values of m and n) and the correct value of the nonlocal elasticity constant e_0 in order to assess the size-effects on buckling loads. This task is undertaken in the next section where MD simulations are used in conjunction with classical and nonlocal models to calculate the values of the aforementioned parameters.

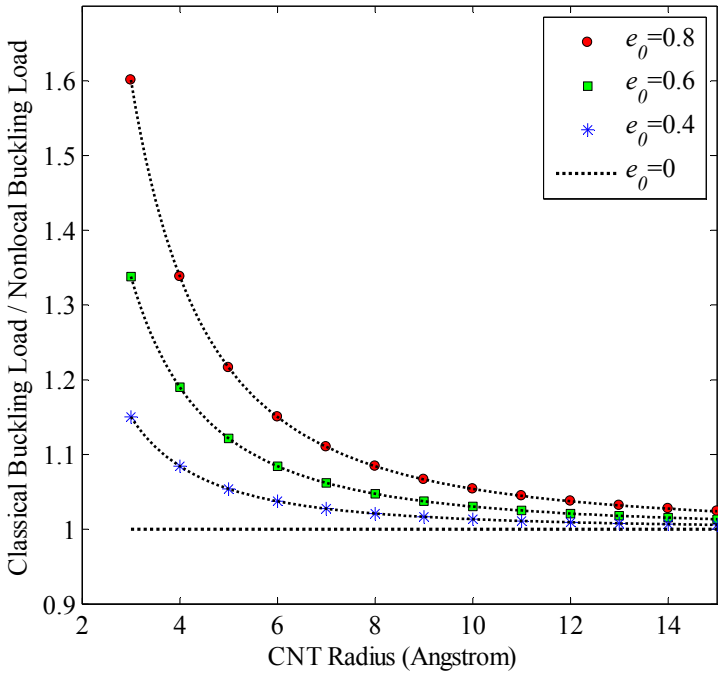

Fig. 3. Comparison of classical and nonlocal buckling loads (equations 17 & 21) for different values of the nonlocal constant e_0 (λ=0.5 and n=2 have been used).

3. Determination of the Nonlocal Constant

It is interesting to compare the nonlocal models derived here with classical models to see if a substantial improvement is achieved in the prediction of CNT buckling loads. Ideally, it is best to compare the axial buckling models with experimental results; however, currently no such experimental results have been reported for SWCNTs. Thus, molecular dynamics is used to simulate the axial buckling of SWCNTs and extract the corresponding buckling loads. Optimized values of shell thickness and nonlocal constant for the axial buckling of CNTs are found and compared with the values previously obtained for torsional buckling of CNTs [7].

3.1. MD Simulation of CNT Axial Buckling

Quasi-static molecular dynamics is used to simulate the shell-type axial buckling (n >1) of several armchair nanotubes. The axial strain is simulated by changing the coordinates of carbon atoms to a compressively strained state (Fig. 4). These new coordinates are then input into the molecular dynamics simulator and the positions of the atoms at both ends of the CNT are fixed to simulate pined-pined boundary conditions. The CNT is then allowed to relax to an equilibrium configuration under the predefined axial strain. The number of relaxation steps required to reach equilibrium depends on the number of atoms in the system and the applied strain. For each carbon nanotube the above simulation is performed for different compressive axial strains, and it is seen that above a certain value of strain, which is identified as the critical strain for axial buckling, the nanotube collapses into a buckled mode-shape when allowed to relax for a sufficient amount of time (Fig. 5).

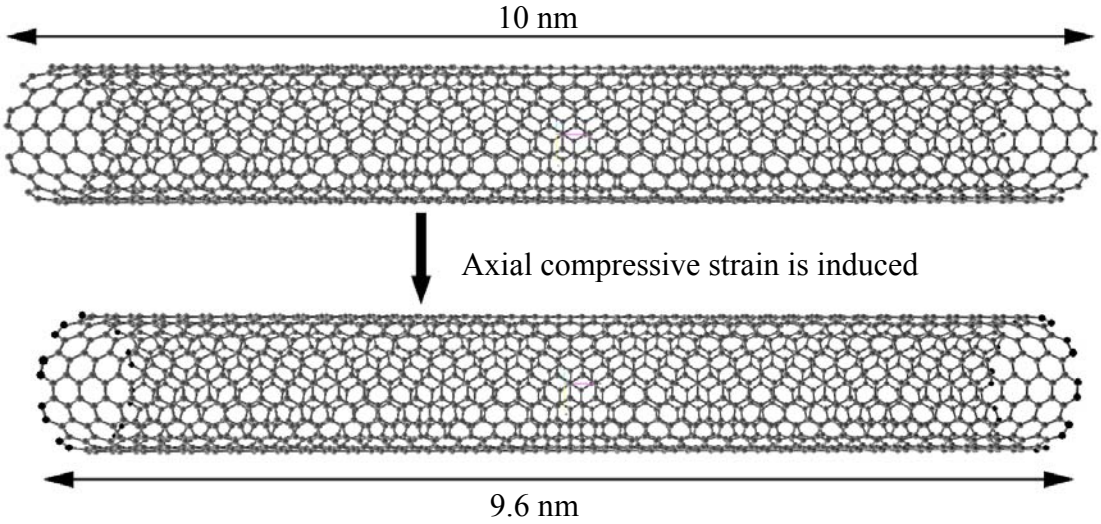

Fig. 4. A compressive axial strain of 0.04 is induced in a (10, 10) armchair CNT by changing the coordinates of carbon atoms (atoms at both ends of CNT shown in dark color are fixed).

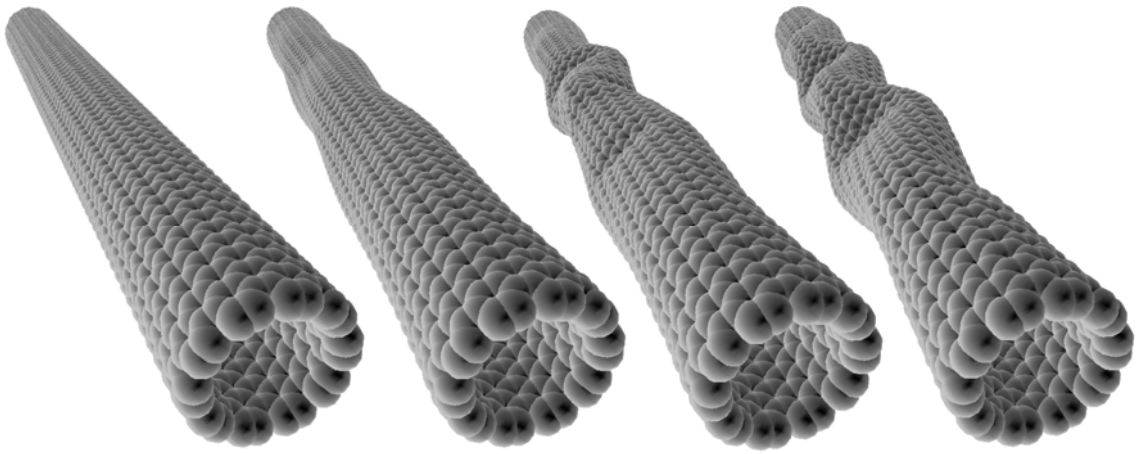

Fig. 5. Different instances of relaxation of a (10, 10) armchair nanotube under an axial compressive strain of 0.04. (a) simulation start; (b) after relaxation for 19250 time-steps; (c) after relaxation for 20250 time-steps; (d) after relaxation for 30000 time-steps.

First, the axial buckling mode-shape calculated with molecular dynamics is compared with the buckling mode-shape of equations (10) and (15) to see if it is correct. As an example, based on equation (15), a (10, 10) armchair nanotube with radius a=6.7 angstroms and length l=163.7 angstroms should have a buckling mode-shape with circumferential wave number n=2 and a longitudinal wave number of $m/2$=2.6. The buckled mode shape of a (10, 10) armchair nanotube at critical strain (0.035) simulated using molecular dynamics is shown in Fig. 6. It is evident that there are two circumferential wavelengths in the transverse direction so that n=2. The number of longitudinal waves can also be counted with a visual inspection of Fig. 6 and is close to $m/2$=2.6 as predicted by the analytical solution.

The progression of the potential energy U of the system with strain ε (Fig. 7) is used to find the compressional stiffness and values of surface Young's modulus. These parameters are needed for use in equations (12) and (13). The surface Young's modulus is found through the following relation:

$$Eh = \frac{1}{2\pi al}\frac{d^2U}{d\varepsilon^2} \tag{24}$$

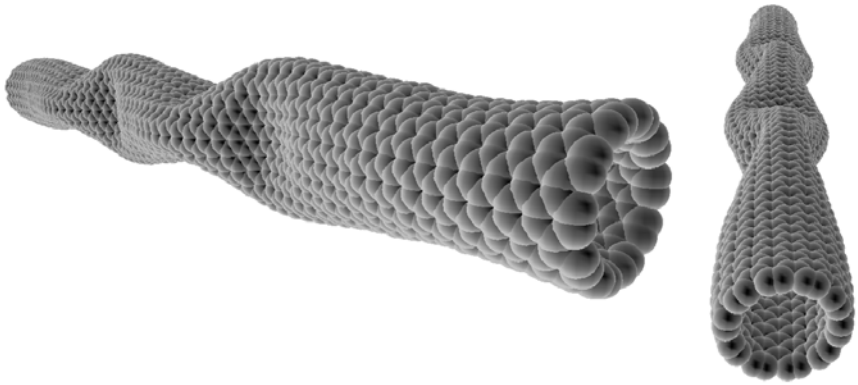

Fig. 6. Axial buckling mode-shape of (10, 10) armchair nanotube at critical strain.

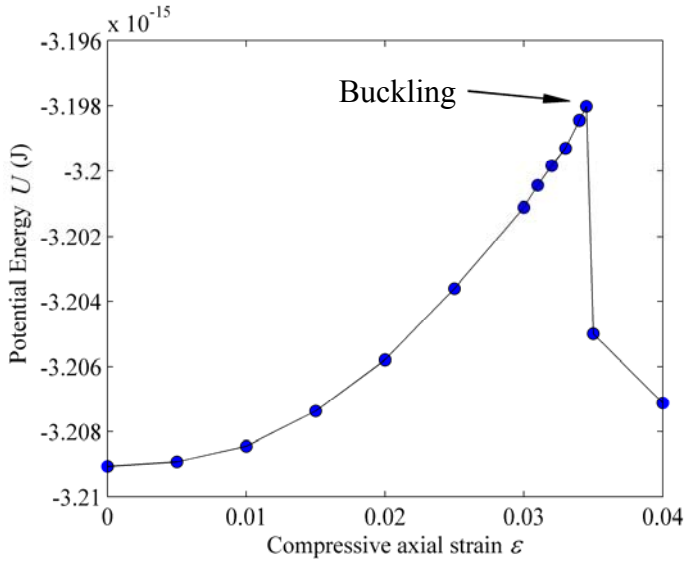

Fig. 7. Progression of potential energy with axial buckling strain of a (10, 10) armchair nanotube.

The critical axial buckling strains and the corresponding critical loads along with the surface Young's moduli of several armchair nanotubes obtained from MD simulations are presented in Table 1.

Table 1. Properties and critical forces and strains of several armchair CNTs.

Chiral Indices	Diam.(Å)	Length L (Å)	L / Diam	$E.h$ (GPa nm)	F_{cr} (N.m)	ε_{cr}	λ_{cr}
(6,6)	8.0	98.21	12.28	323.31	5.68E-08	0.047	0.84
(8,8)	10.7	131.00	12.24	307.93	5.41E-08	0.039	0.72
(10,10)	13.4	163.66	12.21	301.90	5.31E-08	0.035	0.65
(12,12)	16.1	165.00	10.25	299.56	5.26E-08	0.029	0.59
(14,14)	18.8	142.86	7.58	298.03	5.24E-08	0.027	0.54
(16,16)	21.5	160.00	7.44	296.10	5.20E-08	0.024	0.51
(20,20)	26.9	203.84	7.57	295.84	5.20E-08	0.020	0.46

3.4. Values of the Nonlocal Constant and Shell Thickness

A least-squares optimization is performed to calculate the values of parameters to be used in the nonlocal and classical models. The shell thickness h is the optimization variable for the classical case and both shell thickness h and nonlocal constant e_0 are optimization variables for the nonlocal model. The values obtained for these parameters are shown in Table 2.

Table 2. Values of shell thickness (h) and nonlocal constant (e_0).

	h(Å)	e_0	Residual Norm (nN^2)
Classical Timoshenko	0.66	—	196.27
Nonlocal Timoshenko	0.81	0.94	6.66

Looking at the nonlocal model, the optimized values for shell thickness derived from the axial buckling simulations are consistent with the thickness of 0.85 angstroms derived for torsional buckling in the previous work [7] while this is not true for the classical model. The value of the nonlocal elasticity constant derived here is marginally larger than the 0.85 value derived for torsional buckling [7] and the 0.82 value derived by studying the beam type axial buckling of CNTs [8]; however it is within the same range (<15 %). This difference could be attributed to the different deformation fields of the axial and torsional buckling problems, as well as to errors that exist in the numerical simulations.

The results from MD simulations, classical and nonlocal models are compared in Fig. 8. It is seen that for smaller CNTs, the classical model is unable to show the correct trend in critical axial buckling load with change in diameter (Fig. 8(a)) while the nonlocal shell model shows much better agreement with the molecular dynamics simulation results (Fig. 8 (b)).

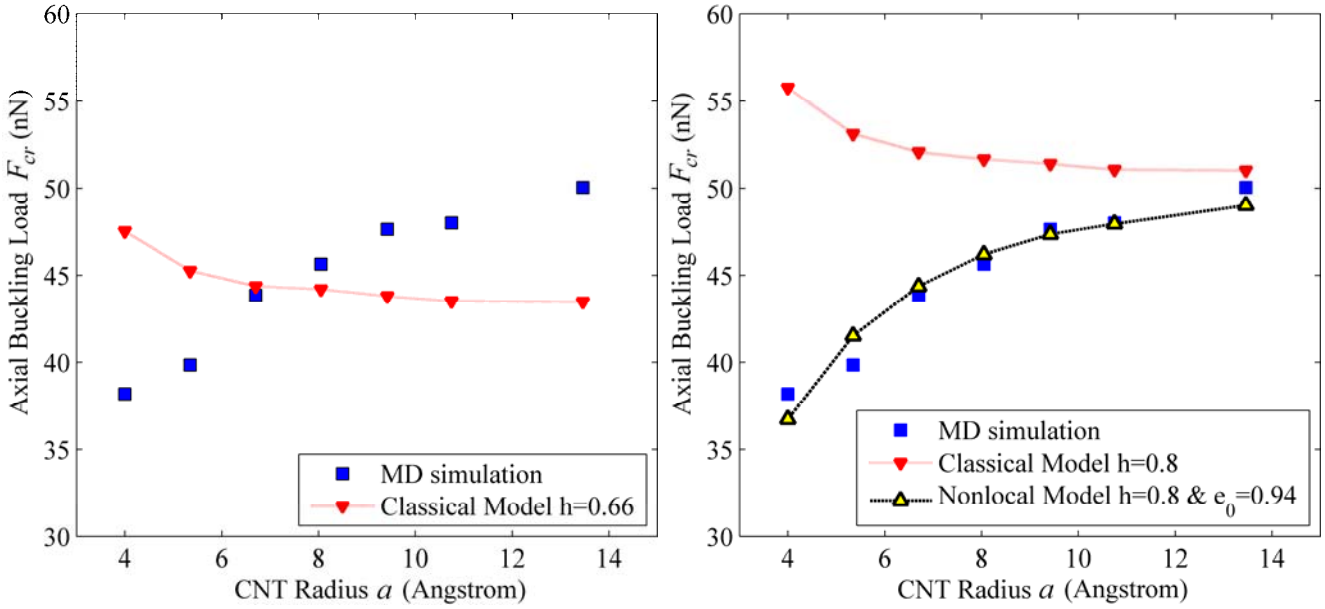

(a) (b)

Fig. 8. Comparison of axial buckling loads from (a) classical and (b) nonlocal shell model with MD results for several armchair CNTs based on properties given in Table 2.

The best match between MD simulations and nonlocal formulations is achieved for a nonlocal constant value of e_0=0.94. Interestingly, for CNTs with small radii (less than 1.5 nm) the classical model predicts axial buckling loads that decrease with the increase in CNT radius (Fig. 8 (a)), while the nonlocal model predicts axial buckling loads that increase with the increase in CNT radius (Fig. 8 (b)), which is the behavior shown by the molecular dynamics simulation results. As seen from Fig. 8 (b), for CNTs with larger radii (larger than 1.4 nm), if used with a shell thickness of h=0.8 Å, the classical model can predict the MD axial buckling loads with good accuracy (the error is less than 5 %).

4. Conclusions

It is found that compared to classical elastic shell models, the modified nonlocal elastic shell model provides a much better fit to MD simulation results (Fig. 8) of axial buckling of SWCNTs. For CNTs with small radii, classical models are unable to show the correct trend in buckling load with the change in CNT radius. This is due to ignoring the size effects. Based on the current study, a global thickness of 0.081 nm for CNTs subject to axial compression is proposed. Value of the nonlocal constant is calculated as 0.94 for axial buckling. Through comparison of classical and nonlocal elasticity models it is concluded that classical approaches overestimate the critical axial buckling loads of CNTs and the error is more significant for CNTs with smaller diameters. For CNTs with large diameters (several nanometers or more), size effects are insignificant and both the classical and nonlocal models predict the same values for the axial buckling load.

Acknowledgements

This work was supported by a grant from the Natural Sciences and Engineering Research Council of Canada.

References

[1]. A. C. Eringen. Linear theory of nonlocal elasticity and dispersion of plane waves, *Int. J. Eng. Sci.,* Vol. 10, Issue 5, 1972, pp. 425-423.
[2]. A. C. Eringen. Screw dislocation in nonlocal elasticity, *Journal of Physics D-Applied Physic.,* Vol. 10, 1977, pp. 671-678.
[3]. A. C. Eringen, On differential equations of nonlocal elasticity and solutions of screw dislocation and surface waves, *J. Appl. Phys.,* Vol. 54, Issue 9**,** 1983, pp. 4703-4710.
[4]. J. Peddieson, G. R. Buchanan, R. P. McNitt, Application of nonlocal continuum models to nanotechnology, *Int. J. Eng. Sci.,* Vol. 41, Issue 3-5, 2003, pp. 305-312.
[5]. Y. Q. Zhang, G. R. Liu, X. Han, Effect of small length scale on elastic buckling of multi-walled carbon nanotubes under radial pressure, *Physics Letters A,* Vol. 349, Issue 5, pp. 370-376.
[6]. S. Timoshenko, J. M. Gere, *Theory of elastic stability*, McGraw-Hill New York, 1961.
[7]. F. Khademolhosseini, N. Rajapakse, A. Nojehz, Determination of nonlocal elasticity constants for the torsional buckling of single-wall carbon nanotubes using molecular dynamics, in *Proceedings of the Conference on 'Biofuels, Renewable Energy, Coatings, Fluidics and Compact Modeling (Nanotechnology 2009),* Houston, USA, 3-7 May 2009*,* pp. 331-334.
[8]. Y. Q. Zhang, G. R. Liu, J. S. Wang. Small-scale effects on buckling of multiwalled carbon nanotubes under axial compression, *Physical Review B,* Vol. 70, Issue 20, 2004, pp. 205430-205437.

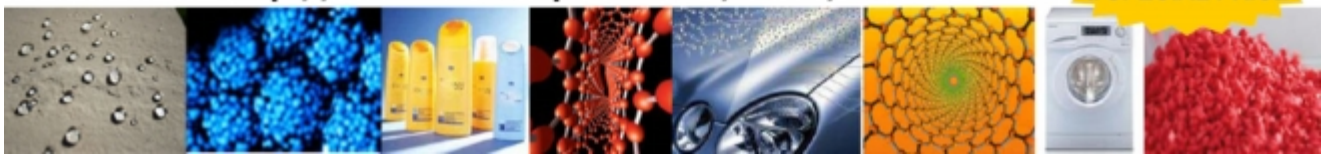

Guide for Contributors

Aims and Scope

Sensors & Transducers Journal (ISSN 1726-5479) provides an advanced forum for the science and technology of physical, chemical sensors and biosensors. It publishes state-of-the-art reviews, regular research and application specific papers, short notes, letters to Editor and sensors related books reviews as well as academic, practical and commercial information of interest to its readership. Because it is an open access, peer review international journal, papers rapidly published in *Sensors & Transducers Journal* will receive a very high publicity. The journal is published monthly as twelve issues per annual by International Frequency Association (IFSA). In additional, some special sponsored and conference issues published annually. *Sensors & Transducers Journal* is indexed and abstracted very quickly by Chemical Abstracts, IndexCopernicus Journals Master List, Open J-Gate, Google Scholar, etc.

Topics Covered

Contributions are invited on all aspects of research, development and application of the science and technology of sensors, transducers and sensor instrumentations. Topics include, but are not restricted to:

- Physical, chemical and biosensors;
- Digital, frequency, period, duty-cycle, time interval, PWM, pulse number output sensors and transducers;
- Theory, principles, effects, design, standardization and modeling;
- Smart sensors and systems;
- Sensor instrumentation;
- Virtual instruments;
- Sensors interfaces, buses and networks;
- Signal processing;
- Frequency (period, duty-cycle)-to-digital converters, ADC;
- Technologies and materials;
- Nanosensors;
- Microsystems;
- Applications.

Submission of papers

Articles should be written in English. Authors are invited to submit by e-mail editor@sensorsportal.com 8-14 pages article (including abstract, illustrations (color or grayscale), photos and references) in both: MS Word (doc) and Acrobat (pdf) formats. Detailed preparation instructions, paper example and template of manuscript are available from the journal's webpage: http://www.sensorsportal.com/HTML/DIGEST/Submition.htm Authors must follow the instructions strictly when submitting their manuscripts.

Advertising Information

Advertising orders and enquires may be sent to sales@sensorsportal.com Please download also our media kit: http://www.sensorsportal.com/DOWNLOADS/Media_Kit_2009.pdf

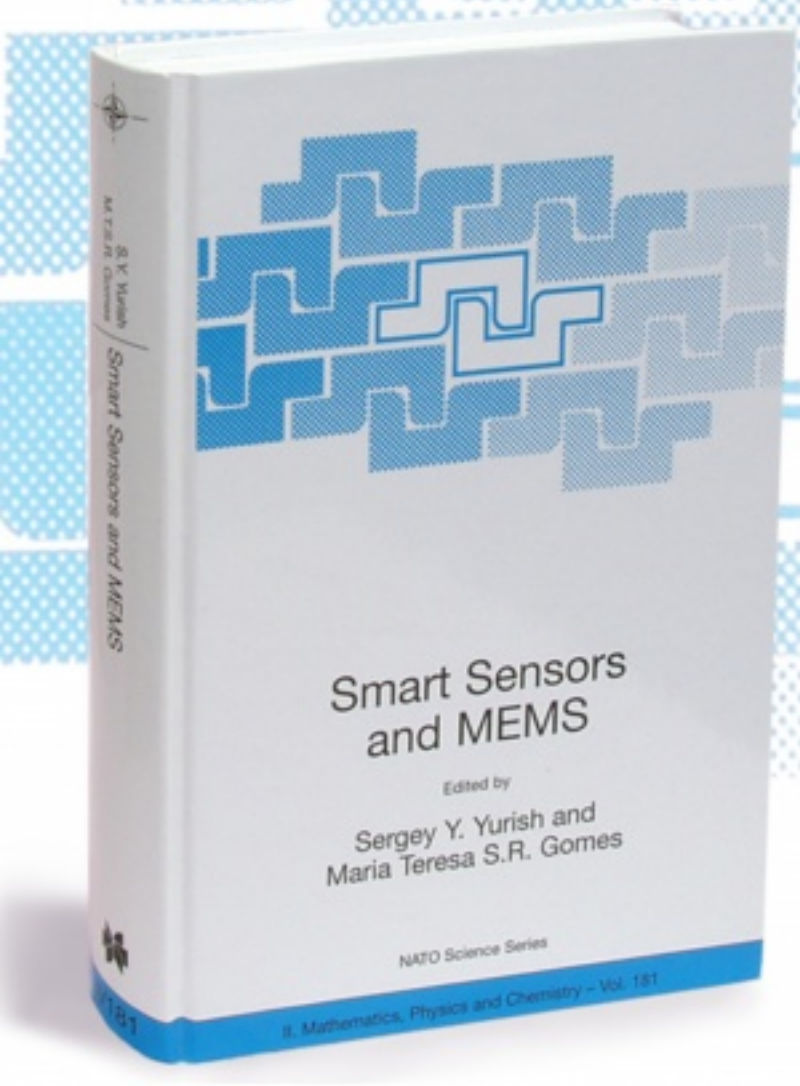

Smart Sensors and MEMS

Edited by

Sergey Y. Yurish and
Maria Teresa S.R. Gomes

The book provides an unique collection of contributions on latest achievements in sensors area and technologies that have made by eleven internationally recognized leading experts ...and gives an excellent opportunity to provide a systematic, in-depth treatment of the new and rapidly developing field of smart sensors and MEMS.

The volume is an excellent guide for practicing engineers, researchers and students interested in this crucial aspect of actual smart sensor design.

Kluwer Academic Publishers